UDC 620.171.3:616.71-001.5-089.227.84
DOI: 10.20535/2521-1943.2020.89.195054

# Spatial deformations of osteosynthesis systems. Message 2. Experimental results

**M. S. Shidlovskiy • M. M. Dyman • O. P. Zakhovaiko • D. G. Odydko**

Igor Sikorsky Kyiv Polytechnic Institute, Kyiv, Ukraine

Received: 23 December 2019 / Accepted: 25 May 2020

***Abstract.*** *Test procedure and a device for the spatial loading of full-scale bone specimens with fractures and fixation means and simultaneous measurement of mutual displacements arising in the fracture region due to the load are presented. The device allows us to apply longitudinal, transverse bending and rotational one-time and long-term cyclic loads to the specimen, simulating the action of loads when walking. The measurement of displacements was carried out by digitally photographing the fracture areas followed by computer image processing.*

*The test results of the "tibia with simulated fracture – fixation plate" systems under spatial loading by three external forces are presented, which cause compression, bending and torsion. As a result of the tests, the values of mutual displacements and the angles of mutual rotation of parts of the fracture were measured.*

*Comparison of test and calculation results using the relationships described in Message 1 shows the suitability of the method, which allows us to quickly and reliably assess the level of displacements in bone fractures under the spatial loading.*

***Keywords:*** *osteosynthesis, biomechanical characteristics, tibia, compression, bending, torsion, displacements in a fracture, angle of rotation, dangerous loads, permissible load.*

## Introduction

Recently, a large number of works, in particular [1 – 5], have been devoted to an experimental study of the reliability of means for fixing bone fractures. Most of these studies are based on methods for measuring displacements in fractures in case of single and short-term external loads, mainly when they act along the longitudinal axis of the bone, less often when bending. The combined influence of the forces operating in most of the possible directions is hardly considered, although in our opinion this case is the most important from a practical point of view (walking, treatment procedures, etc.).

## Block-and-lever device for the complex loading of osteosynthesis (OS) systems

For an experimental study of the spatial displacements of points in fracture area and mutual angles of rotation of parts of bone, a device has been designed and created that allows the simultaneous action of compressive, bending, and rotational loads on the system of "bone with a fracture – means of fixation". A general view of the device is shown in Fig. 1, *a*, and its spatial model is presented in Fig. 1, *b*.

The device is intended for applying static and cyclic loads when testing OS tools with the simultaneous action of compression, bending and torsion. In the process of loading at every moment of time, it is possible to digitally photograph the fracture area and further determine the displacements (mutual displacements) of points of the opposite parts of the fracture [6 – 9].

✉ M. S. Shidlovskiy
n_shidlovsky@ukr.net

✉ M. M. Dyman
hateandhope@mail.ru

✉ O. P. Zakhovaiko
zakhov1911@gmail.com

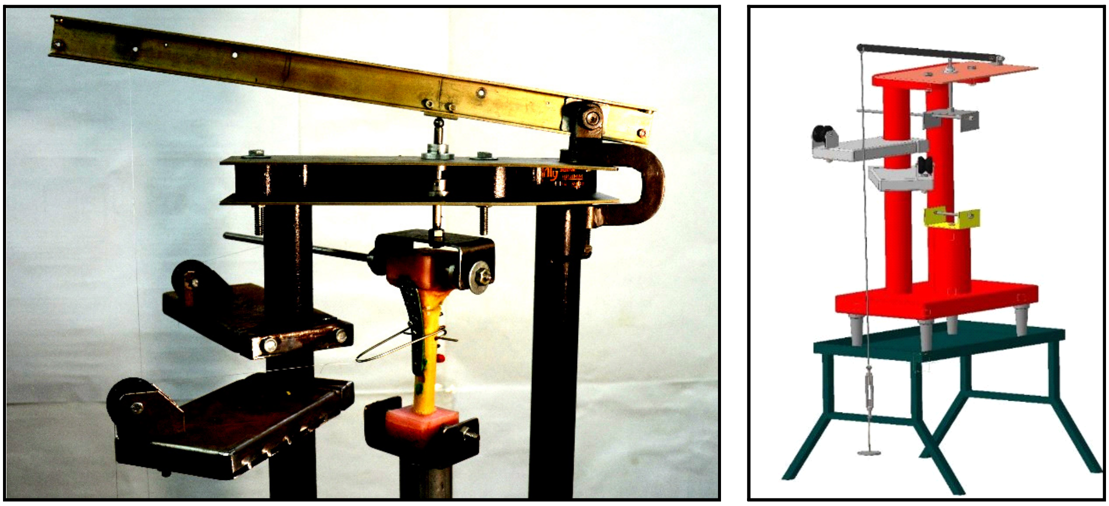

*a* *b*

**Fig. 1**. The device for complex loading of the system “bone with a fracture – fixing plate” (*a*) and its spatial model (*b*)

### The principle of operation of the device

The experimental device consists of the following main units (Fig. 2): unit for fixing the specimen “bone with a simulated fracture – means of fixation”; unit for loading the bone in compression; unit for loading bones by bending; a unit for applying torque to the bone; lever system for cyclic loading.

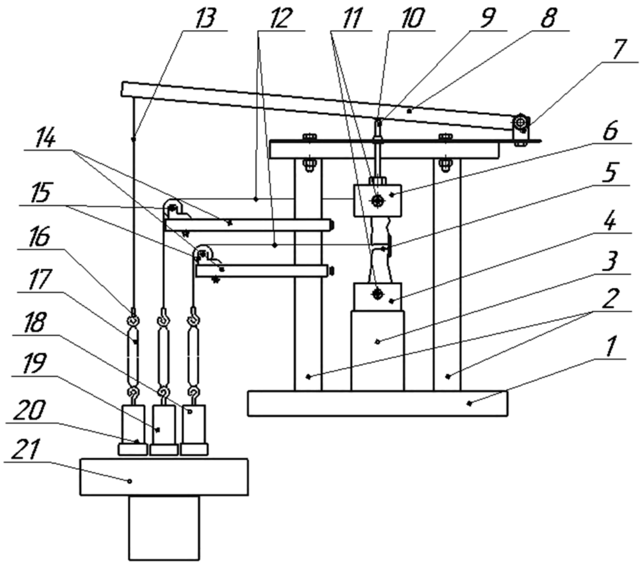


**Fig. 2.** The scheme of a test device for the study of osteosynthesis systems under complex loading

In Fig. 2 we see: *1* – Fixed frame; *2* – Supporting columns; *3* – Lower support; *4* – Lower clamp; *5* – Specimen; *6* – Upper clamp; *7* –Hinge; *8* – Lever; *9* – Loading rod; *10* –Ball; *11* –Axis; *12* and *13* – Ropes; *14* – Stands for blocks; *15* – Replaceable blocks; *16* –Hook; *17* – Lanyard; *18* – Weight to create bend; *19* – Weight to create torsion; *20* – Weight to create compression; *21* – Loading unit.

The weight *20* creates compression loading. This load is transmitted through the lanyard *17* and the flexible rope *13* to the lever *8*. This lever loads the rod *9*, which is rigidly connected to the movable upper clamp *6*. The upper clamp carries an axial compressive load on the specimen *5*.

The bending load is created by the weight *18* using the rope *12*, thrown over the block *15*. The rope is attached to the specimen *5* and creates a bending moment.

The torsion is created by the weight *19* which transfers the load to the upper movable clamp *6* through the second block *15* using the rope *12*. This rope is fixed to the special rod in upper clamp *6* set perpendicularly to the longitudinal axis of the specimen.

The TIRA-test universal testing machine was used to lift and lower three weights *18*, *19*, *20* and to perform one-time or repeated loading. To do this, a lever attached to the movable cross-arm of the testing machine is used. A plate is attached to the right edge of the lever, which performs lifting and lowering the load. The cyclic load modes (number of cycles, load speed and frequency, other cycle characteristics) are set by the control unit of the testing machine.

Device features are: application of compression loads in the range from 10 to 800 N; application of bending loads in the range from 10 to 200 N; application of rotational torque in the range from 2 to 20 N·m; cyclic loads in the indicated ranges with a frequency of 1 … 5 $s^{-1}$; determination of linear displacements of fracture parts in different directions during loading with an accuracy of ±0.02 mm; determination of rotation angles of fracture parts in different planes with an accuracy of ±0.1°; determination of irreversible displacement of fracture parts under the action of static and cyclic loads.

Control tests were performed using the tibia with a simulated fracture, which was fixed with a medial blocked straight plate. A detailed description of the plate, the method of manufacturing samples and preparation for testing is provided in [10, 11].

Fig. 3 shows the photo of one of studied test specimens and the direction of action of forces and moments under spatial loading. The generalized data on geometry of specimens and the loads are given in Table 1. The tests were carried out using three identical specimens of tibia with simulated fractures, which were fixed by these plates.

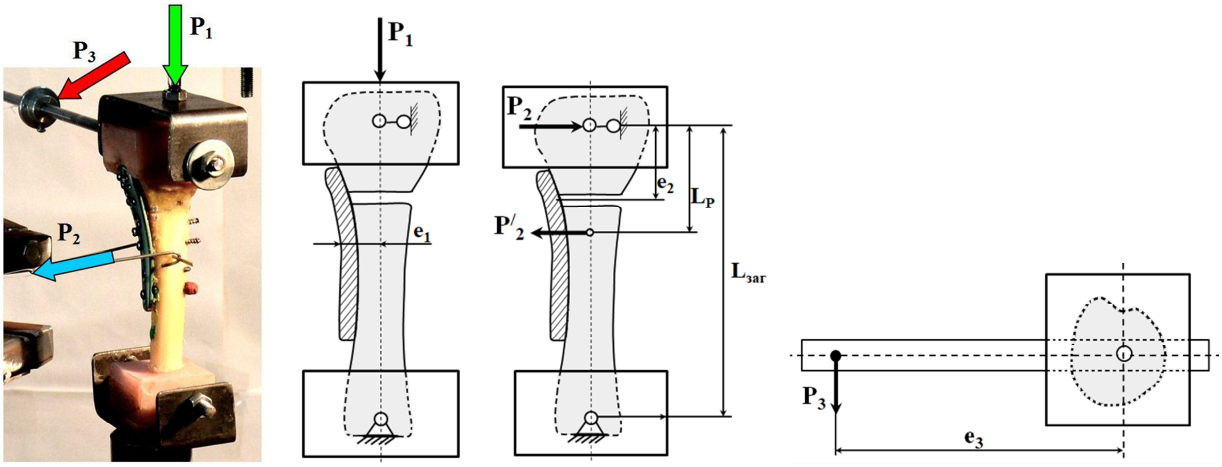


**Fig. 3.** Directions of the loads applied to the bone during their joint action (*a*) and separate loads under compression (*b*), bending (*c*) and torsion (*d*)

**Table 1.** The loads and geometrical characteristics of tibia specimens with fractures, which were fixed by plates, and subject to joint action of compression, bending and torsion

| Characteristic | | Value |
|---|---|---|
| Axial load (compression) | $P_1$ | 147.1 N |
| Transverse load (bending) | $P'_2$ | 49.1 N |
| Lateral force (reaction in the upper support) | $P_2$ | 28.5 N |
| Rotational load | $P_3$ | 5.88 N |
| Distances from the line of action of the force to the place of fixation of the fracture | $e_1$ | 17.5 (±0.5) mm |
| | $e_2$ | 32.0 (±0.8) mm |
| | $e_3$ | 215 (±1.5) mm |
| Distance between supports (bend) | $L_{total}$ | 146 (±0.5) mm |
| The distance from the upper support to the point of application of force | $L_P$ | 61.2 (±0.5) mm |
| Fracture size (distance between the medial point *M* and the lateral point *L*) | $S_{ML}$ | 29.0 (±0.5) mm |

### Results of experimental determination of displacements

After applying the loads $P_1$, $P_2$ and $P_3$, the displacements of the fracture points $\Lambda^L$ and $\Lambda^M$ were measured in the maximum distance from the plate (point *L*) and near the plate (point *M*) by digital photography. The measurement results are given in Table 2 (the method I). The indices *X, Y, Z* denote the projections of the total displacements on the corresponding axes (*X* is the longitudinal axis of the bone, *Y* is the axis perpendicular to the *X*-direction and parallel to the plane of the plate, *Z* is the axis perpendicular to the *X* and *Y* axes).

**Table 2.** Displacements of the fracture points *L* (farthest from the plate) and *M* (near the plate) when fractures were fixed with the «3M» plate

| The point and the direction of displacement | | Method I | Method II | Relative difference Δ, % |
|---|---|---|---|---|
| Farthest from the plate lateral point *L* | $\Lambda^L_X$, mm | 2.09 | 2.20 | 5.00 |
| | $\Lambda^L_Y$, mm | 1.48 | 1.53 | 3.26 |
| | $\Lambda^L_Z$, mm | 0.46 | 0.49 | 6.12 |
| Total displacement of point $\Lambda^L$, mm | | 2.60 | 2.72 | 4.41 |
| Near the plate medial point M | $\Lambda^M_X$, mm | 0.67 | 0.70 | 4.29 |
| | $\Lambda^M_Y$, mm | 0 | 0 | – |
| | $\Lambda^M_Z$, mm | 0.46 | 0.49 | 6.12 |
| Total displacement of point $\Lambda^M$, mm | | 0.80 | 0.85 | 5.88 |
| The angle of rotation of parts of the fracture Γ, …° | | 4.05 | 4.23 | 4.25 |

*Note: the Method I: data were obtained by direct measurement of displacements under the joint action of forces P1, P2 and P3;*
*Method II - calculation results which were defined using experimental data obtained at separate loading.*

In this table the full mutual displacements of two fracture points are given as the geometric sums of the three components:

$$\Lambda^L = \sqrt{\left(\Lambda_X^L\right)^2 + \left(\Lambda_Y^L\right)^2 + \left(\Lambda_Z^L\right)^2}\,; \tag{1}$$

$$\Lambda^M = \sqrt{\left(\Lambda_X^M\right)^2 + \left(\Lambda_Y^M\right)^2 + \left(\Lambda_Z^M\right)^2} \tag{2}$$

and the angle of mutual rotation of the parts of the fracture, calculated by the formula

$$\Gamma_{\max} = \arccos\left[1 - \frac{\left(\lambda_X^L - \lambda_X^M\right)^2 + \left(\lambda_Y^L - \lambda_Y^M\right)^2 + \left(\lambda_Z^L - \lambda_Z^M\right)^2}{2S_{ML}^2}\right]. \tag{3}$$

### Comparative calculations

To check the results of the three-dimensional loading, analytical calculations of displacements of the fracture points and rotation angles of fracture parts were carried out using the data obtained by testing under the action of separate compression, bending and torsion (See Message 1.).

The displacement components for the lateral (farthest from the plate) fracture points *L* and the medial (near the plate) fracture points *M* were calculated using the formulas

$$\Lambda_j^L = \sum_{k=1}^{3} P_k (\lambda_{jk}^L + \bar{\lambda}_{jk}^L \cdot e_k)\,; \tag{4}$$

$$\Lambda_j^M = \sum_{k=1}^{3} P_k (\lambda_{jk}^M + \bar{\lambda}_{jk}^M \cdot e_k)\,. \tag{5}$$

Total displacements of these points according to the formulas

$$\Lambda^L = \sqrt{\sum_{j=1}^{3}\left[\sum_{k=1}^{3} P_k(\lambda_{jk}^L + \bar{\lambda}_{jk}^L \cdot e_k)\right]^2}\ ; \tag{6}$$

$$\Lambda^M = \sqrt{\sum_{j=1}^{3}\left[\sum_{k=1}^{3} P_k(\lambda_{jk}^M + \bar{\lambda}_{jk}^M \cdot e_k)\right]^2}\ . \tag{7}$$

In the expressions (4) – (7) $\lambda_{jk}^i = \dfrac{\Lambda_{jk}^i}{P_k}$ and $\bar{\lambda}_{jk}^i = \dfrac{\Lambda_{jk}^i}{M_k}$ shows the displacements, the values of which were obtained when specimens were separately tested for compression, bending and torsion. Here *j* is the designation of the axes (*X, Y* or *Z*); *k* = 1, 2, 3 is the number of forces. Force moments are defined as $M_k = P_k \cdot e_k$.

Table 3 shows the values of these coefficients calculated for the system “tibia with a fracture – fixing plate”.

**Table 3.** The displacements $\lambda_{jk}^i \times 10^3$, mm/N and $\bar{\lambda}_{jk}^i \times 10^3$ mm/(N·mm) of the fracture points *L* (farthest from the plate) and *M* (near the plate) when fractures were fixed with the «3M» plate

| | $\lambda_{Xk}^L$ | $\lambda_{Yk}^L$ | $\lambda_{Zk}^L$ | $\bar{\lambda}_{Xk}^L$ | $\bar{\lambda}_{Yk}^L$ | $\bar{\lambda}_{Zk}^L$ |
|---|---|---|---|---|---|---|
| *k* = 1 | 4.75 | 0 | 0 | 0.429 | 0 | 0.134 |
| *k* = 2 | 0 | 0 | 0.64 | 0.427 | 0 | 0.134 |
| *k* = 3 | 0 | 0 | 0 | 0 | 1.213 | 0 |
| | $\lambda_{Xk}^M$ | $\lambda_{Yk}^M$ | $\lambda_{Zk}^M$ | $\bar{\lambda}_{Xk}^M$ | $\bar{\lambda}_{Yk}^M$ | $\bar{\lambda}_{Zk}^M$ |
| *k* = 1 | 4.75 | 0 | 0 | 0 | 0 | 0.134 |
| *k* = 2 | 0 | 0 | 0.64 | 0 | 0 | 0.134 |
| *k* = 3 | 0 | 0 | 0 | 0 | 0 | 0 |

The values of the forces $P_1$, $P_2$, $P_3$ and the geometric characteristics of the system (distances $e_1$, $e_2$, $e_3$) in the calculations are taken to be the same as in the experiments (Table 1). The results of determining the mutual displacements of the parts of the tibia fracture fixed by a medial blocked straight plate are given in table 2 (method II).

The table 2 shows the relative difference between the data obtained by the described methods:

$$\Delta = \frac{\left|\Lambda_{jk(I)}^i - \Lambda_{jk(II)}^i\right|}{\Lambda_{jk(II)}^i} \cdot 100\ \%\ . \tag{8}$$

Based on the data of the table 2, a satisfactory match between the data obtained in two ways can be noted. Note that in all cases the results of calculations using the data of separate loadings and reduced displacements slightly exceed the results of measuring displacements under the simultaneous action of loads $P_1$, $P_2$ and $P_3$. This is due to some mutual influence of these forces and a decrease in actual loads due to friction in the units of the block-and-lever device. In general, the differences in the indicators measured in two ways lies within 3 – 6 %, which is at the level of measurement error.

The data presented confirm the suitability of calculation methods for estimating allowable loads (see Message 1), since the value of displacements and rotation angles calculated using the reduced displacements $\lambda_{jk}^i = \Lambda_{jk}^i / P_k$ and $\bar{\lambda}_{jk}^i = \Lambda_{jk}^i / M_k$, measured at separate loadings, correspond to real ones, those that arise with three-dimensional complex loadings. This, in turn, confirms the suitability of using maximum displacement of fracture points or maximum angles of mutual rotation and relevant criterion relations as the functional reliability criteria for determining allowable loads (See Formulas (1), (2), (4), (6) given in Message 1).

The described methods for determining displacements in osteosynthesis systems provide an opportunity to quickly and reliably assess the level of displacements in bone fractures, fixed in different ways, under the spatial force system. At the same time, it is possible to determine the contribution of each component of loads to the general level of displacements and the angle of rotation of the fracture parts and, due to this, to determine the dangerous directions of the loads and their acceptable levels.

## Conclusions

1. A device has been designed and created that allows loading full-scale bone specimens simultaneously with axial and transverse force and torque. In this case, the method of digital photography can measure the displacement of various fracture points in different planes and directions.
2. Tests were performed to measure the spatial displacements of the lateral (most distant) fracture point under complex loading (compression, bending and twisting). The comparison of test results with calculations performed using simple test data (separate action of compression, bending and torsion), showed a satisfactory match between the results.
3. The proposed method makes it possible to accelerate comparative estimates of the rigidity of different systems of osteosynthesis on full-scale specimens with simulated fractures or using artificial models made of synthetic materials.

## References


1. Weber T.G. The role of fibular fixation in combined fractures of the tibia and fibula: a biomechanical investigation / Weber T.G., Harrington R.M., Henley M.B., Tencer A.F. // J Orthop. Trauma. – 1997. – Vol. 11, No. 3. – P. 206–211.
2. Zelle B.A. Treatment of distal tibia fractures without articular involvement: a systematic review of 1125 fractures / Bhandari M., Espiritu M., and dr. // J Orthop Trauma. – 2006. – Vol. 20, No. 1. – P. 76–79.
3. Jaarsma R.L. Rotational malalignment after fractures of the femur/van Kampen A. // J Bone Joint Surg Br. – 2004. – Vol. 86, No. 8. – P. 1100–1104. https://doi.org/10.1302/0301-620X.86B8.15663
4. Ricci W.M. Angular malalignment after intramedullary nailing of femoral shaft fractures. / Bellabarba C., Lewis R., and dr. // J Orthop Trauma. – 2001. – Vol. 15, No. 2. – P. 90–95.
5. Tonin M.S. Biomechanical systems of osteosynthesis in the treatment of clavicle fractures : Author’s thesis. S.: 2009. – 22 p.
6. Шидловського М.С., Лакши А.М. Експериментальні дослідження засобів остеосинтезу. – К.: Ленвіт, 2017. – 277 с.
7. Патент на корисну модель № 68177. Спосіб вимірювання зміщень уламків кісток людини в експерименті. Шидловський М.С., Радомський О.А., Літун Ю.М., Аксютін А.Г. Зареєстровано 12.03.2012 р., Бюл. № 5, 2012.
8. Патент на корисну модель № 117085. Спосіб визначення зміщення уламків кісток в місцях переломів / Шидловський М.С., Заховайко О.П., Димань М.М. Зареєстровано 12.06.2017 р., Бюл. № 11, 2017.
9. Патент на корисну модель № 128638 Спосіб вимірювання просторових переміщень уламків кісток людини в експерименті / Шидловський М.С., Літун Ю.М., Заховайко О.П., Онищенко Є.Є., Димань М.М. Зареєстровано 25.09.2018 р., Бюл. № 18, 2018.
10. Бур’янов О.А., Шидловський М.С., Омельченко Т.М., Димань М.М., Мусієнко О.С. Деформаційні характеристики систем фіксації, що застосовуються при переломах та корекційних остеотоміях дистального відділу великогомілкової кістки // Літопис травматології та ортопедії. – 2017. – № 1–2. – С. 129–133.
11. Shidlovskiy M., Dyman M., Omelchenko T. The tibial fractures fixation system deformation characteristics // Mechanics and Advanced Technologies. – 2018. – Vol. 84, No. 3. – P. 52–60. https://doi.org/10.20535/2521-1943.2018.84.141615


# Просторове деформування систем остеосинтезу. Повідомлення 2. Експериментальні результати

**М. С. Шидловський, М. М. Димань, О. П. Заховайко, Д. Г. Одудько**

***Анотація.*** *Представлені методика випробувань та пристрій для просторового навантаження натурних зразків кісток з переломами та засобами фіксації і одночасним вимірюванням взаємних зміщень, що виникають в переломах в результаті дії цих навантажень. Пристрій дозволяє прикладати до зразка поздовжні, поперечні згинальні та ротаційні одноразові та довготривалі циклічні навантаження, що моделює дію системи навантажень при ходьбі. Вимірювання переміщень проводили шляхом цифрового фотографування областей перелому з подальшою комп’ютерною обробкою зображень.*

*Наведено результати тестових випробувань систем “великогомілкова кістка з модельованим переломом – фіксуюча пластина” при просторовому навантаженні трьома зовнішніми силами, що викликають стиск, згин та кручення. В результаті випробувань виміряні величини взаємних переміщень та кути взаємного повороту частин перелому.*

*Співставлення результатів випробувань та розрахунків з використанням співвідношень, описаних в Повідомленні 1, показало придатність методу, що дає можливість оперативно та достовірно оцінювати рівень переміщень в переломах кісток під дією просторової системи сил.*

***Ключові слова:*** *остеосинтез, біомеханічні характеристики, великогомілкова кістка, стиск, згин, кручення, переміщення в переломі, кут повороту, небезпечні навантаження, допустиме навантаження.*

# Пространственное деформирование систем остеосинтеза. Сообщение 2. Экспериментальные результаты

**Н. С. Шидловский, М. М. Дымань, А. П. Заховайко, Д. Г. Одудько**

***Аннотация.*** *Представлены методика испытаний и устройство для пространственной нагрузки натурных образцов костей с переломами и средствами фиксации и одновременным измерением взаимных смещений, возникающих в переломах в результате действия этих нагрузок. Устройство позволяет прикладывать к образца продольные, поперечные изгибающие и ротационные одноразовые и долговременные циклические нагрузки, что моделирует действие системы нагрузок при ходьбе. Измерения перемещений проводили путем цифрового фотографирования областей перелома с последующей компьютерной обработкой изображений.*

*Приведены результаты тестовых испытаний систем "большеберцовая кость с моделированным переломом - фиксирующая пластина" при пространственной нагрузке тремя внешними силами, что вызывают сжатие, изгиб и кручение.*

*В результате испытаний измеренные величины взаимных перемещений и углы взаимного поворота частей перелома.*

*Сопоставление результатов испытаний и расчетов с использованием соотношений, описанных в Сообщении 1, показало пригодность метода, что дает возможность оперативно и достоверно оценивать уровень перемещений в переломах костей под действием пространственной системы сил.*

***Ключевые слова:*** *остеосинтез, биомеханические характеристики, большеберцовая кость, сжатие, изгиб, кручение, перемещения в переломе, угол поворота, опасные нагрузки, допустимая нагрузка.*

## References

1. Weber, T.G., Harrington, R.M., Henley, M.B. and Tencer, A.F. (1997), "The role of fibular fixation in combined fractures of the tibia and fibula: a biomechanical investigation", *J Orthop. Trauma,* vol. 11, no. 3, pp. 206–211.
2. Zelle, B.A., Bhandari, M., Espiritu, M. and dr. (2006), "Treatment of distal tibia fractures without articular involvement: a systematic review of 1125 fractures", *J Orthop Trauma,* vol. 20, no. 1, pp. 76–79.
3. Jaarsma, R.L. van Kampen, A. (2004), "Rotational malalignment after fractures of the femur", *J Bone Joint Surg Br.*, vol. 86, no. 8, pp. 1100–1104. https://doi.org/10.1302/0301-620X.86B8.15663
4. Ricci, W.M., Bellabarba, C., Lewis, R., and dr. (2001), "Angular malalignment after intramedullary nailing of femoral shaft fractures", *J Orthop Trauma*, vol. 15, no. 2, pp. 90–95.
5. Tonin, M.S. (2009), *Biomehanicheskie sistemyi osteosinteza pri lechenii perelomov klyuchitsyi* [Biomechanical systems of osteosynthesis in the treatment of clavicle fractures], avtoref. dis., Saratov, Russian.
6. Shidlovskogo, M.S. and Lakshi, A.M. (ed.) (2017), *Eksperimentalni doslidzhennya zasobiv osteosintezu*, [Experimental studies of osteosynthesis], Lenvit, Kyiv, Ukraina.
7. Shidlovskiy, M.S., Radomskiy, O.A., Litun, Y.M., AksyutIn, A.G. Zareestrovano 12.03.2012, Byul. № 5, 2012, Sposib vimiryuvannya zmischen ulamkiv kistok lyudini v eksperimentI, Patent na korisnu model № 68177.
8. Shidlovskiy, M.S., Zahovayko, O.P., Diman, M.M. 12.06.2017, Byul. № 11, 2017, Sposib viznachennya zmischennya ulamkiv kistok v mistsyah perelomiv, Patent na korisnu model № 117085.
9. Shidlovskiy, M.S., Litun, Y.M., Zahovayko, O.P., Onischenko, E.E., Diman, M.M. 25.09.2018, Byul. № 18, 2018, Sposib vimiryuvannya prostorovih peremischen ulamkiv kistok lyudini v eksperimenti, Patent na korisnu model № 128638.
10. Bur'yanov, O.A., Shidlovskiy, M.S., Omelchenko, T.M., Diman, M.M., Musienko, O.S. (2017), "Deformatsiyni harakteristiki sistem fiksatsiyi, scho zastosovuyutsya pri perelomah ta korektsIynih osteotomiyah distalnogo viddilu velikogomilkovoyi kistki", *Litopis travmatologiyi ta ortopediyi*, no. 1–2, pp. 129–133.
    Shidlovskiy, M., Dyman, M. and Omelchenko, T. (2018), "The tibial fractures fixation system deformation characteristics", *Mechanics and Advanced Technologies*, vol. 84, no. 3, pp. 52–60. https://doi.org/10.20535/2521-1943.2018.84.141615